Experimental investigation on ablation-assisted current interruption – Experimental setup and preliminary results

Henning Taxt, Kaveh Niayesh
Department of Electrical Engineering
Norwegian University of Science and Technology
Trondheim, Norway
henning.taxt@ntnu.no

Erik Jonsson, Magne Runde
Department of Electric Power Technology
SINTEF Energy Research
Trondheim, Norway
magne.runde@sintef.no

***Abstract*— This paper presents a flexible setup to investigate ablation-assisted interruption of load currents. The electrical test circuit is grid connected with a transformer secondary voltage from 6.9 kV to 24 kV. The applied stress to the switching device, such as load current amplitude and transient recovery voltage amplitude and shape, can be set to a large range of values by adjusting the circuit components–resistors, reactors and capacitors–in fine steps.**

A parallel capacitive-resistive voltage divider ensures high bandwidth and low offset voltage measurements. A resistive shunt is used for current measurement and, in addition, a post-arc current sensor is dedicated to the exact measurement of currents lower than 3 A. The high quality of the measurements allows for a detailed study of the extinction voltage peak, current trace prior to current zero and the post-arc current.

Load current interruption measurements from one forced airflow switch and two ablation switches are presented and compared. The ablation switches have a clear current limiting effect close to current zero, whereas the air switch gives a linear decline of the current to zero. One of the ablation switches sustains a post-arc current for 7 ms, without experiencing a re-ignition.

Keywords—experimental setup; post-arc current; ablation; medium voltage; load-break switch

I. INTRODUCTION

The urge to replace SF_6, without driving up size and cost, is nowadays an important driver for further development of medium voltage switchgear. The improved utilization of polymer ablation for arc quenching is one of the promising technologies that could contribute to such a development [1]. Ablation-assisted current interruption is no new technology, and a range of products utilized this effect from early 1900s and onwards [1-5]. However, a good description of their performance and limitations, as well as a thorough physical explanation of the arc quenching properties, especially for lower currents, is lacking in literature.

Ablation-dominated static arcs, which is a valid assumption in the high current region, have been described [6-9]. However, from a current interruption perspective, the arc behaviour in the high current region is not necessarily the most important phenomenon. In [10], the authors try to determine which measures are most suited for evaluating interruption performance in a low voltage circuit breaker. They conclude that their macroscopic evaluators, such as 10-ms arc energy, maximum and mean voltages, and maximum and mean currents, are not very useful for evaluating interruption performance. On the other hand, their microscopic evaluators, for example conductivity and current the first microseconds after current zero, are in general suited for evaluating interruption performance.

The extinction of ablation-dominated arcs has not been thoroughly described in literature. Jonsson et al. [11] present some experimental results under low voltage conditions, suggesting that high hydrogen content in the ablation gas is beneficial. Onchi et al. [12] have calculated the decay in temperature and conductivity around current zero for different polymers, and present it in 10-µs time steps. This gives valuable insight into the mechanisms contributing to a fast decay in conductivity.

As shown, the fast processes near current zero are decisive for the interruption performance of a switch. In order to evaluate properly the interruption capability of medium voltage ablation switches, it is critical to get high-quality measurements in the tens of microseconds around current zero. This paper presents a complete experimental setup for the investigation and development of medium voltage ablation switches. In the next section, the electrical test circuit is presented, followed by a description of the measurement system and the contact driving mechanism. To demonstrate the adequacy of the experimental setup, results from experiments with two different ablation switches are presented, together with a reference measurement from a forced airflow switch experiment.

II. ELECTRICAL TEST CIRCUIT

The electrical test circuit is designed to provide, in essence, the same stress on the test object as the tests described as "mainly active load current duty" in IEC 62 271-103, i.e. the same current and transient recovery voltage (TRV) up to the first peak. The rationale, further elaborated in [13], is that the test duties in the standard, ranging from 7.2 kV to 52 kV, can be replicated using a relatively inexpensive transformer.

The electrical circuit is supplied from the 11.4-kV utility grid via a 600-kVA transformer. The transformer has been

This work is part of a research project supported by the Research Council of Norway and ABB Norway.

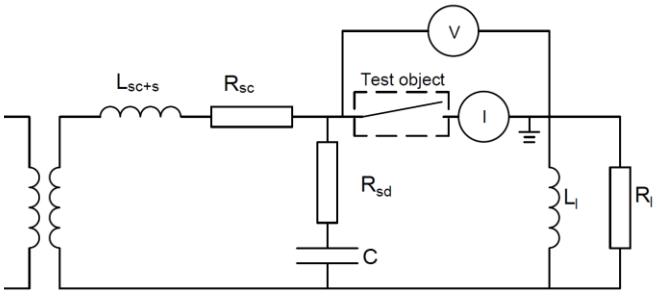

Fig. 1. Electrical test circuit for load-break switch development

constructed with two sets of secondary windings that can be connected in parallel or series. In addition, the secondary windings can be connected in delta or star configuration, resulting in four available source voltages – 6.9, 12, 13.8 and 24 kV.

The main network components in the test circuit are shown in Fig. 1. All the components can be set to a large range of values, and can be adjusted in small steps in order to fine-tune the current and TRV shape. A detailed description is given in [13]. Calculating the resulting current in the circuit is trivial, and is depending on the source voltage, source-side inductor, load inductor and load resistor. The exact calculation of the TRV amplitude and shape on the other hand, is more laborious. The TRV is first simulated in ATP Draw to find the values of the circuit components. The circuit is then tested to see if the correct current, TRV amplitude, rate of rise of recovery voltage (RRRV) and voltage shape are produced. The parameters of the circuit elements are then adjusted if necessary.

In the present setup, the circuit elements are configured to give a current of 600 A_{rms}, a first peak amplitude of TRV of 5 kV and a RRRV of 120 V per µs. The source voltage is 6.9 kV. The TRV is evaluated when the circuit is interrupted by an air switch without ablation effect. As the ablation switch changes the arc-circuit interaction, and the circuit is unchanged, the resulting TRVs can become different. The values set for the network components are given in Table 1.

TABLE I. NETWORK COMPONENT VALUES IN THE PRESENT EXPERIMENTS

Component	Symbol	Value
Source-side inductor [a]	L_s	12.33 mH
Source side resistor [b]	R_s	1.24 Ω
Capacitor	C	0.032 µF
Damping resistor	R_{sd}	190 Ω
Load inductor	L_l	32.52 mH
Resistance of load inductor	R_{Ll}	1.73 Ω
Load resistor	R_l	13.05 Ω

[a.] : Includes transformer inductance

[b.] Sum of transformer and source-side inductor resistance

III. MEASUREMENT SETUP

A. Data link and acquisition system

All experiments are monitored and controlled from a control room. The measurement signals are transferred to the control room by means of fibre optic links with bandwidth from DC to 12.5 MHz and 12-bit resolution. The fibre optic transmitter's analogue input is selectable; ±1 V or ±5 V. The fibre optic receiver's analogue output is ±5V. The signal is finally collected to a computer with a NI-2110 and NI-6110 PCI, with 12-bit resolution and 5 MS/s. The analogue input has a bandwidth of 4.8 MHz.

B. Arc voltage measurement

The voltage measurement should have sufficient resolution and bandwidth to detect details in arc voltage, especially around current zero, and measure the slope and amplitude of the transient recovery voltage (TRV) after current zero with high precision. It is crucial to have a reliable detection of zero voltage.

The arc voltage is measured with a parallel capacitive-resistive voltage divider. The resistive part dominates in the low frequency range and enables a correct zero voltage detection, whereas the capacitive divider gives a good high-frequency response. The voltage ratio is the same for both the resistive and the capacitive divider parts. The impedance of the divider is sufficiently high to make the influence on the test circuit negligible. The high voltage resistor is 480 kΩ and the high voltage capacitor is 208 pF. The capacitor branch has a damping resistor of 200 Ω to avoid high-frequency oscillations.

The low voltage part of the divider is interchangeable with three different sets of impedances giving the following voltage ratios: 1:600, 1:2000 and 1:6000. The response is linear within 3dB from low frequencies and up to more than 1 MHz. For voltage measurements, the divider is the component limiting the bandwidth.

C. Current measurement

Two different sensors are used for current measurement, one for measuring in the high-current region and another to measure the current close to zero with high precision. For the high-current region, an inductance-free 2.5-mΩ shunt resistor is used.

In the study of arc interruption phenomena, there is a need for exact measurement of the current around current zero, as this is when the decisive processes governing the success or failure of the thermal interruption takes place. It is not practical to measure both regions with the same sensor, so for the measurement of small currents, a post-arc current sensor was built in-house. The sensor is based on the one described in [15]. A 50-mΩ shunt is by-passed by diodes when the current is high. In the low current region, the diodes are not conducting, and the voltage over the resistive shunt is linear with the current.

The transition between the open and closed states of the diodes is critical for the performance of this sensor. The current level at which the transition takes place is determined by the forward voltage drop of the diodes and the resistance of the shunt. To ensure a swift transition, Schottky diodes are used. They offer a low capacitance and practically no reverse recovery time. The shunt and the diodes are placed in a co-axial layout in

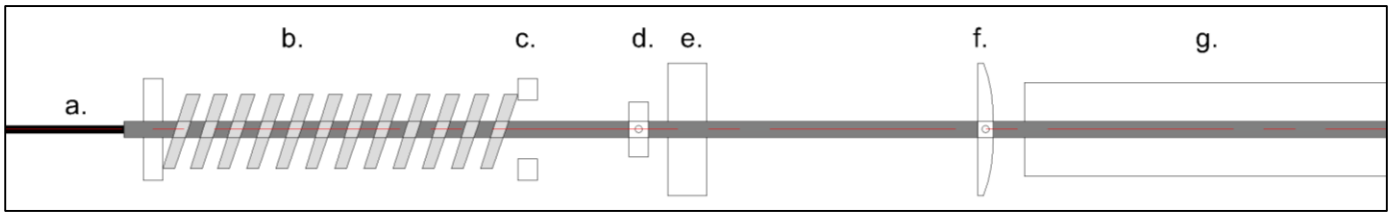

Fig. 2 The mechanical driving mechanism in open position. The pin contact (a) is fastend to a movable shaft. The spring (b) is hold in place by c. In the closed position, the spring (b) is armed by (d), which is fasted to the movable shaft, as the shaft is in its far-left position. The shaft is hold in the armed position by the electromagnet (e) that atracts the steel plate (f). The movment is measured by means of the linear potentiometer (g).

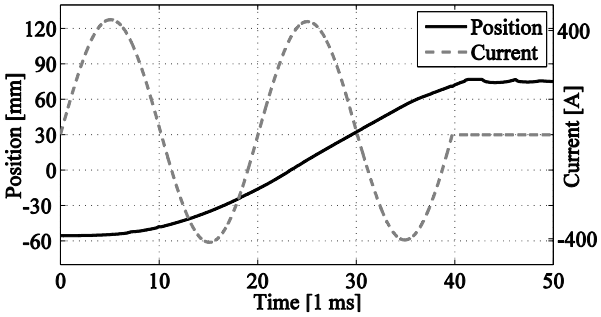

Fig. 3 Example travel curve for a switch similar to switch C.

order to reduce parasitic inductance that would increase the transition time and negatively affect the measurement.

The two current signals are merged in a post-processing procedure. For any current lower than 3 A the signal from the post-arc current sensor is used, and for any other value of the current, the signal from the shunt is used. At low values, close to 3 A, the signal from the shunt is small –only a few times the least significant bit– and becomes noisy. The signal from the shunt is therefore smoothed with a Savitsky-Golay filter, with a moving evaluation window of 4 µs, and using second order polynomials. No filter is applied to the signal from the post-arc current sensor.

D. Contact driving mechanism and position measurement

The driving mechanism is shown in Fig. 2. The movement of the contact pin is driven by a pre-charged spring that is held in place by an electromagnet. Switching off the magnet releases the moving contact and initiates its movement, in a reproducible manner and synchronized with respect to the source voltage. The force of the spring can be adjusted. In the experiments presented here, contact speed is around 5 m/s. The contact travel is recorded by means of a linear potentiometer, giving a signal from 1 to 4 V. An example travel curve is shown in Fig. 3.

IV. INITIAL EXPERIMENTAL RESULTS

A. Parallel-plate ablation switch

Initial tests have been conducted to compare the voltage and current characteristics of different switch designs, shown in Fig. 4, and to verify the setup's ability to measure accurately. Switch A is similar to the one presented in [16], but with some modifications. This is a parallel-plate arrangement where ablation of polypropylene (PP) contributes to quenching the arc. The plates are 70 mm in the direction of the contact movement, 30 mm of height and are placed 4 mm apart. The two short sides and the bottom is closed, so that the arcing chamber is open only upwards. The pin diameter is 4 mm and the contact gap at end position is 65 mm.

An air switch is used as a reference for the experiment. Fig. 5 shows the measured currents and voltages for the parallel-plate ablation switch (A) and the air switch (B). In addition, the resulting conductance for switch A is shown – the signal is smoothed from t = -10 µs to t = 10 µs to suppress the unreliable and high values when the voltage is approaching its zero crossing. The conductance of switch B is not shown here, but it is straightforward to see that it drops about 15 µs later than for switch A, and that it goes linearly to zero – or a very low value – about 3 µs before voltage zero crossing. The time from this abrupt decrease in conductance to the voltage zero crossing, is simply a result of the arc voltage and circuit the elements.

The most obvious difference between switch A and B, is the higher arc voltage of switch A, 650 V in switch A and around 200 V in switch B, in the high current region (not shown in the figure). Close to current zero, the arc voltages increase to about 500 V for the air switch B and 1500 V for the ablation switch A. The distinct voltage peak in switch A is a result of its rapidly decreasing conductance. The current is limited by the switch and can be seen as a new rate of change of current below 5 A. The interaction with the circuit forces the voltage to increase.

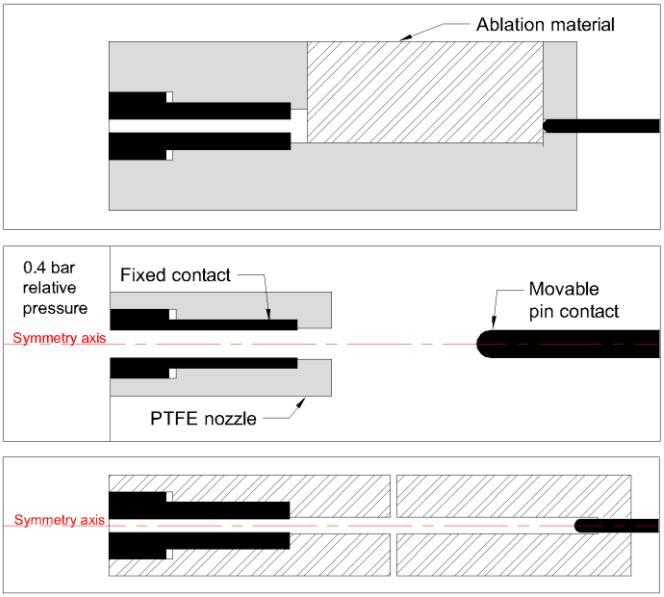

Fig. 4 Drawing of the three switches A (top), B (middle) and C (bottom) in open position. Solid black parts are tungsten-copper contacts, solid grey are PTFE and areas with stripes show ablation material.

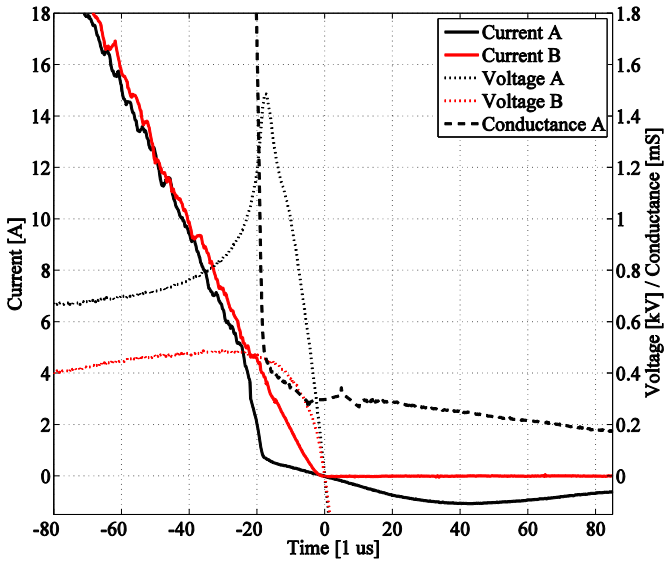

Fig. 5 Voltage and current measurements for an ablation switch (A) and an air switch (B) in an identical electrical circuit. The conductance of the contact gap is calculated and shown for A, smoothed to suppress the unreliable and high values when voltage is close to zero.

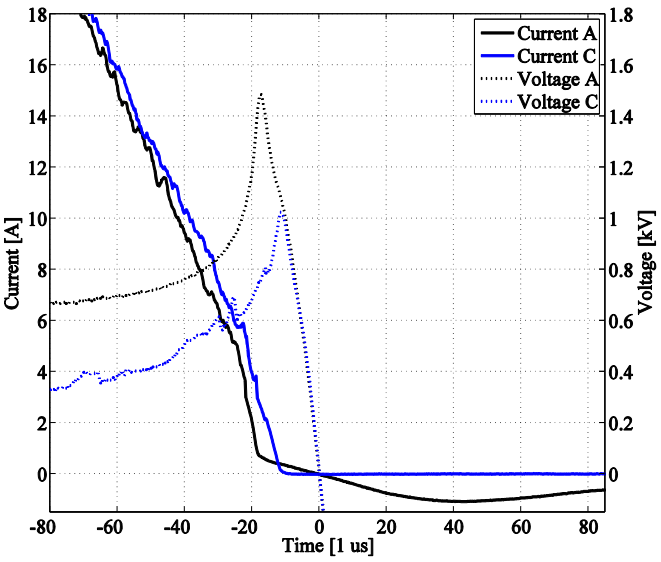

Fig. 6 Voltage and current measurements for ablation switch (A) as in Fig. 5 and another ablation switch (C) with a tubular arc chamber and more restricted arc in an identical electrical circuit.

Another feature by ablation switch A, is the residual conductance of 400 µS after the arc is apparently extinguished, about 18 µs before current zero crossing. From that point, the conductance decreases slowly. 100 µs after current zero crossing it is 150 µS and it reaches 10 µS about 700 µs after current zero. The conductance then increases and decreases again until the next current zero crossing occurs after about 7 ms, without resulting in a full restrike. The first peak of the post-arc current of 1.1 A appears after 42 µs. A second peak comes after 3.1 ms, with a value of 0.2 A. Such a long period of post-arc current could indicate that some kind of energy balance is reached in this case, and that this switching is on the borderline to fail. The mechanisms causing such a long-lasting post-arc current have not been investigated here, but possible explanations include high conductance along the surface of the arcing chamber or some hot gas or hot electrode phenomena. In studies of low voltage circuit breakers, a similar long-lasting post-arc current has been reported, with explanation that a glow discharge can keep the current running [17]. More typically, post-arc currents are present for shorter periods, from a few microseconds and up to a few hundred microseconds [15, 18].

B. Tubular ablation switch

Tests have been conducted on a different ablation switch (C) as shown in Fig 4. The arcing chamber is a 90-mm long tube with an inner diameter of 5 mm. As the moving contact pin moves in this tube, away from the fixed contact, the arc is elongated in this volume. A 2-mm section of the tube, at a distance of 30 mm from the fixed contact, is removed. This opening in the tube serves as a gas outlet and as a physical barrier to ensure that current cannot flow on the surface between the electrodes.

Fig. 6 shows an example of current interruption measurement with switch C in an identical electric circuit as the experiments in Fig. 5. The contacts are 40 mm apart when the current is interrupted. Two main differences between switches A and C can easily be pointed out:

- Switch A provides a significantly higher arc voltage than switch C, and this leads to an earlier decay in current.
- Switch C has zero, or a very low, post-arc current, which significantly improves the thermal interruption capability of switch C compared to switch A.

Even though the post-arc current sensor is not able to detect any post-arc current in this case, a small current could still be present – the least significant bit is 10 mA. To investigate this properly, the sensitivity of the post-arc current sensor could be further improved, by increasing the shunt resistance or amplifying the sensor's output signal. However, considering the heating of the post-arc channel, the significance of this small post-arc current is probably limited. In the case of switch A, the maximum power dissipation in the post-arc channel is about 5 kW, whereas for switch C it is less than 50 W.

V. DISCUSSION AND CONCLUSION

In this paper, a direct test setup with precise current and voltage measurement systems has been presented. This is intended for investigation of the thermal phase of load current interruption in medium voltage load break switches.

The electrical test circuit is designed to generate load current and voltage stress similar to the IEC testing procedure for "mainly active load current duty", up to the first peak of the TRV. The measurement system is able to detect all relevant voltages and, more importantly, currents in both the high-current region and near current zero.

First measurements show the significant impact of the arc voltage on the current flowing through the load break switch, especially near current zero. This is of particular importance if load break switches with a strong ablation effect are evaluated.

The initial experiments also reveal that the ablation switch, depending on design, can sustain a post-arc current for quite a long time. A maximum post-arc current of 1.1 A has been observed, along with durations, though at a lower current, of up to half a power cycle. A post-arc current of such a magnitude and duration is generally an unwanted feature in a medium voltage switch, because it increases the risk of a thermal runaway and re-ignition.

Future work on this experimental setup will include systematic investigations of the interruption performance of ablation switches. Tests should be carried out with different current and voltage stresses and with changes in switch geometry, in order to identity the most important arc-quenching mechanisms.

ACKNOWLEDGEMENTS

I want to thank the laboratory service personnel at the Norwegian University of Science and Technology for help during this work.

REFERENCES

[1] Taxt, H., *Ablation-assisted current interruption in medium voltage switchgear – Development and prospect (unpublished)*, in *24th Nordic Insulation Symposium on Materials, Components and Diagnistics*. 2015: Copenhagen, Denmark.

[2] Mayr, O., *Ein neuer Leistungstrennschalter*. ETZ, 1935. **56**(44): p. 1189-1192.

[3] Petermichl, F., *Hartgasschalter.* AEG Mitteilungen, 1938(Heft 11): p. 521-523.

[4] Keuneke, W., *Hartgasschalter.* AEG Mitteilungen, 1957. **47**(7/8): p. 285-288.

[5] Rawlins, H.L., *Load break disconnect*. 1943, Google Patents.

[6] Niemeyer, L., *Evaporation Dominated High Current Arcs in Narrow Channels.* Power Apparatus and Systems, IEEE Transactions on, 1978. **PAS-97**(3): p. 950-958.

[7] Ibrahim, E.Z., *The ablation dominated polymethylmethacrylate arc.* Journal of Physics D: Applied Physics, 1980. **13**(11): p. 2045.

[8] Gonzalez, D., H. Pursch, and F. Berger, *Experimental investigation of the interaction of interrupting arcs and gassing polymer walls.* 2011 Ieee 57th Holm Conference on Electrical Contacts, 2011.

[9] Ruchti, C.B. and L. Niemeyer, *Ablation Controlled Arcs.* Plasma Science, IEEE Transactions on, 1986. **14**(4): p. 423-434.

[10] Balestrero, A., et al., *Current interruption in low-voltage circuit breakers.* Power Delivery, IEEE Transactions on, 2010. **25**(1): p. 206-211.

[11] Jonsson, E., et al., *Comparative Study of Arc-Quenching Capabilities of Different Ablation Materials.* IEEE Transactions on Power Delivery, 2013. **28**(4): p. 2065-2070.

[12] Onchi, T., Y. Tanaka, and Y. Uesugi, *Effect of polymer ablation gas on arc quenching properties around current zero.* Electrical Engineering in Japan, 2012. **180**(3): p. 32-45.

[13] Jonsson, E. and M. Runde, *Medium voltage laboratory for load break switch development*, in *Int. Conf. Power Syst. Transients, Vancouver, BC, Canada*. 2013.

[14] *Hartgasschalter (Kompressorlose Druckgasschalter).* AEG Mitteilungen, 1938(Heft 3): p. 181-182.

[15] Barrault, M., et al., *Post-arc current measurement down to the ten milliamperes range.* IEEE Transactions on Power Delivery, 1993. **8**(4): p. 1782-1788.

[16] Gjendal, G.J., E. Jonsson, and M. Runde. *Ablation-Assisted Current Interruption in a Medium Voltage Load Break Switch*. in *ICEC 2014; The 27th International Conference on Electrical Contacts; Proceedings of*. 2014. Dresden, Germany.

[17] Hauer, W. and X. Zhou. *Re-ignition and Post Arc Current Phenomena in Low Voltage Circuit Breaker*. in *ICEC 2014; The 27th International Conference on Electrical Contacts; Proceedings of*. 2014.

[18] Ghezzi, L. and A. Balestrero, *Modeling and Simulation of Low Voltage Arcs*, Thesis. 2010, TU Delft, Delft University of Technology.